Response of Air Cushion Vehicles to Random Seaways and the Inherent Distortion in Scale Models

D. R. Lavis* and R. J. Bartholomew†
Aerojet-General Corporation, Tacoma, Wash.
and
J. C. Jones‡
Aerojet-General Corporation, Sacramento, Calif.

The heave, pitch, and roll equations of motion for an Air Cushion Vehicle are derived. The dynamic response to a random seaway is predicted from the linearized perturbation equations and compared with experimental tests of a subscale dynamically similar model operating in a towing tank. Frequency domain seakeeping analysis to determine acceleration response, frequency of bow slamming, structural loads, and relative motion between two craft is demonstrated. Because the atmosphere is not scaled during subscale model tests, an appreciable dynamic distortion is reflected in lift system physical parameters. This scaling problem is discussed and avenues of further subscale model experimental research are suggested.

Nomenclature

V_B = cushion volume
A_B = cushion area
C = cushion periphery
L = cushion length
l_b = distance from c.g. to bow
l_s = distance from c.g. to stern
C_{Do} = fixed area airflow discharge coefficient
C_{DS} = heave dependent leakage area airflow discharge coefficient
C_B = adiabatic stiffness $(\bar{p}_B + P_A)\gamma / V_B$
R_l = fan conductance
F_c = fan characteristic slope $(\partial \bar{Q}_F / \partial \bar{p}_B)$
G = heave dependent leakage parameter $G = C_{DS} C (2\bar{p}_B/\rho_A)^{1/2}$
ρ_A = atmospheric air density
P_A = atmospheric pressure
γ = ratio of specific heats for air
m = ratio of distance from c.g. to bow to total length
m_c = uniform distribution part of mass of craft per unit length
W_j, W_s, W_{sj} = discrete weights at longitudinal station x_j; lateral station y_s, or at (x_j, y_s), respectively
M_c = total mass of craft
M_f = mass of suddenly removed weight for step input excitation
x_f = longitudinal distance of M_f from c.g.
y_f = lateral distance of M_f from c.g.
I_θ = pitch moment-of-inertia of craft
I_φ = roll moment-of-inertia of craft
d_z = heave damping derivable from measured pitch damping = $3d_\theta / L^2(1 - 3m + 3m^2)$
d_θ = pitch damping = $2\zeta_\theta (I_\theta K_\theta)^{1/2}$
d_φ = roll damping = $2\zeta_\varphi (I_\varphi K_\varphi)^{1/2}$
ζ_θ = pitch damping ratio, measured from tests
ζ_φ = roll damping ratio, measured from tests
K_θ = pitch spring rate = $K_{\theta D}[(L^3/3)(1 - 3m + 3m^2]$, measured from tests
K_φ = roll spring rate = $K_{\varphi D} B^3/12$, measured from tests
$K_{\theta D}$ = distributed pitch spring rate
$K_{\varphi D}$ = distributed roll spring rate
$S_o(\omega)$ = wave amplitude power spectral density
ω = absolute wave frequency
ω_e = encounter frequency
η_o = wave amplitude, zero to peak

Presented as Paper 72-598 at the AIAA/SNAME/USN Advanced Marine Vehicles Meeting Annapolis, Md., July 17–19, 1972: submitted September 8, 1972; revision received February 5, 1974.

Index categories: Marine Vessel Design (Including Loads); Marine Vessel Systems; Surface Marine Vessel Trajectories, Stability and Control.

*Manager, Technology, Surface Effect Ships Division.

†Associate Scientist, Surface Effect Ships Division. Member AIAA.

‡Engineering Specialist, Liquid Rocket Company.

$[A]$ = mass matrix
$[B]$ = damping matrix
$[C]$ = stiffness matrix
z = linearized heave displacement
θ = linearized pitch displacement
φ = linearized roll displacement
m_B = linearized cushion mass
P_B = linearized cushion pressure
$(\cdot)$ = first derivative with respect to time, velocity
$(\cdot\cdot)$ = second derivative with respect to time, acceleration
U = craft velocity
U_m = model velocity
g = gravitational constant = 32.2 ft/sec^2
i = $(-1)^{1/2}$, index
j,r,s = indices
Z = heave in nonlinear equations of motion
p_B = cushion pressure in nonlinear equations of motion
Θ = pitch in nonlinear equations of motion
Φ = roll in nonlinear equations of motion
M_B = cushion mass in nonlinear equations of motion; bending moment
ρ_B = cushion density
V_o = cushion unloaded volume
Q_F = fan flow rate
Q_{LO} = fixed area leakage airflow rate
A_{LO} = fixed leakage area
Q_{LS} = heave dependent leakage airflow rate
ξ = longitudinal coordinate dummy variable
η = transverse coordinate dummy variable; wave amplitude
$V(x)$ = longitudinal shear force distribution
$M_B(x)$ = longitudinal bending moment distribution
$T(x)$ = longitudinal torsion moment distribution
$V(y)$ = transverse shear distribution
$M_B(y)$ = transverse bending moment distribution
P_{sJO} = joint probability of impact at a given relative velocity of bow
FSB_i = frequency of occurrence of slamming of bow at given relative velocity
h_{ci} = height of bow above level water surface at normal operating condition
v_{si} = given slam relative velocity
σ_i = rms amplitude of bow motion relative to water surface
σ_i' = rms vertical velocity to bow relative to water surface
$S_o(t)$ = unit step function at $t = 0$

Introduction

THE vertical acceleration response (which strongly influences ride comfort and structural loads) has been predicted theoretically by mathematical models for a large ACV and measured experimentally during tests of a subscale dynamically similar model operating in a towing tank. This paper is concerned principally with the aspect of utilizing subscale models to predict the dynamics of

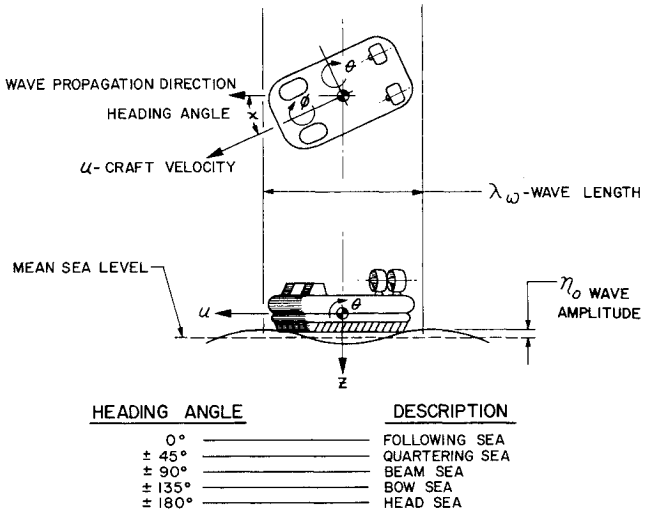

Fig. 1 Description of wave and craft geometry.

full-scale craft. Theoretical and experimental results are compared and use of frequency domain seakeeping analysis is demonstrated. It has been found that because the atmosphere is not scaled during subscale model test, there exists an appreciable distortion in vertical plane dynamic response to the extent that, under certain conditions, the subscale model underpredicts the acceleration environment of the full-scale craft. The particular parameters affecting this "distortion" are discussed in terms of a simple linear heave/cushion flow mathematical model in the frequency domain. The characteristic equation for this model is a cubic polynominal equation in the Laplace operator. The effects of varying certain physical parameters are discussed in terms of the roots of this polynominal equation to determine the damping and natural frequency of the quadratic factor. The cabin acceleration response of a full-scale craft, including pitch effects, is also predicted considering the same changes in physical parameters. Suggested avenues of further experimental research employing subscale models are given, in which the distortion effects of the unscaled atmosphere are minimized or corrected.

Approach to Simulation

Method and Assumptions

The mathematical model of the dynamic behavior of an ACV in the pitch, heave, roll, and cushion flow degrees of freedom is derived from mechanics in accordance with the coordinate system of Fig. 1. The surge motion is neglected, and pitch and roll angles and angular velocities are considered small. For motion over waves, the assumption of a long crested waveform is made, and the craft heading is described by the angle χ as shown in Fig. 1. The wave amplitude (zero to peak from mean sea level) η_o is also shown. It is also assumed that the wave system is not affected by the presence of the craft.

The nonlinear equations of motion are derived in the Appendix. These equations are then linearized by a linear perturbation technique. For wave induced excitations, the equations are transformed into the frequency domain via the Fourier transform, and the solutions are obtained in the form of transfer functions of the ratio of each variable to wave amplitude. For statistical excitations, the Response Amplitude Operators (RAO's) for all three motion variables and auxiliary acceleration variables are obtained from the squares of the amplitude ratios of the transfer functions. Other parameters such as seakeeping loads (longitudinal and transverse bending moment and torsion moment) are obtained as functions of the basic heave, pitch, roll, and cushion pressure transfer functions.

Homogeneous Equations

In matrix form, the linear, homogeneous, coupled, heave-pitch-roll-cushion mass flow, equations of motion are

$$[A]\begin{Bmatrix}\ddot{z}\\ \ddot{\theta}\\ \ddot{\varphi}\\ \ddot{m}_B\end{Bmatrix}+[B]\begin{Bmatrix}\dot{z}\\ \dot{\theta}\\ \dot{\varphi}\\ \dot{m}_B\end{Bmatrix}+[C]\begin{Bmatrix}z\\ \theta\\ \varphi\\ m_B\end{Bmatrix}=0 \quad (1)$$

The inertia matrix $[A]$ is of the form

$$[A]=\begin{bmatrix}M_c & 0 & 0 & 0\\ 0 & I_\theta & 0 & 0\\ 0 & 0 & I_\varphi & 0\\ 0 & 0 & 0 & 0\end{bmatrix} \quad (2)$$

The damping matrix $[B]$ is of the form

$$[B]=\begin{bmatrix}d_z & -d_z(m-0.5)L & 0 & 0\\ -d_z(m-0.5)L & d_\theta & 0 & 0\\ 0 & 0 & d_\varphi & 0\\ 0 & 0 & 0 & 1\end{bmatrix} \quad (3)$$

The stiffness matrix $[C]$ is of the form

$$[C]=\begin{bmatrix}K_{\theta D}L+C_BA_B^2 & -(K_{\theta D}L+C_BA_B^2)(m-0.5)L & 0 & \frac{C_BA_B}{\rho_A}\\ -(K_{\theta D}L+C_BA_B^2)(m-0.5\,L) & K_\theta+C_BA_B^2(m-0.5)^2L^2 & 0 & -\frac{C_BA_B}{\rho_A}(m-0.5)L\\ 0 & 0 & K_\varphi & 0\\ -\rho_A(C_BA_BR_1+G) & \rho_A(C_BA_BR_1+G)(m-0.5)L & 0 & -C_BR_1\end{bmatrix} \quad (4)$$

From matrices (2-4) it is seen that roll is completely uncoupled from the other variables. This happens because the c.g. is taken to be always along a longitudinal line bisecting the cushion. For the special case where the ratio m of longitudinal distance from c.g. to bow l_b to total cushion length L is 0.5, the heave and pitch equations are also uncoupled. In addition to Eq. (1), we have the cushion pressure perturbation P_B given by

$$P_B=(C_B/\rho_A)\,m_B+C_BA_Bz-C_BA_B(m-0.5)L\theta \quad (5)$$

Forcing Functions

Time Domain

For simulation in the time domain, the forcing functions considered were restricted to suddenly applied disturbance forces and moments. During actual model tests, these forces and moments were applied by suddenly removing a weight from the craft. This approximates a step function loading applied to the model in the heave, pitch, and roll degrees of freedom. The vector of applied heave force, pitch moment, and roll moment applied to the right-hand side of Eq. (1) is of the following form:

$$\{F_s\}=M_fgS_o(t)\begin{Bmatrix}-1\\ x_f\\ y_f\\ 0\end{Bmatrix} \quad (6)$$

Frequency Domain

A complex waveform may be characterized by the following form for wave amplitude

$$\eta(x,y,t)=\eta_o e^{-i(k_xx+k_yy-\omega_et)} \quad (7)$$

where the wave surface frequency components are

$$k_x = (\omega^2/g)\ \cos\chi,\ k_y = (\omega^2/g)\ \sin\chi \tag{8}$$

and the wave encounter frequency ω_e is a function of wave frequency ω and craft speed (U) as follows:

$$\omega_e = \begin{cases} (1-\alpha)\omega, & \alpha < 1 \\ -(1-\alpha)\omega, & \alpha \geq 1 \end{cases} \qquad \alpha = (U\omega/g)\cos\chi \tag{9}$$

In the derivation of the nonlinear equations of motion given in the Appendix, the displacement of the wave comes into the equations of motion through the heave, cushion flow, and cushion volume equation, because the displacement relative to the wave surface is required in those equations. The integration of the wave of Eq. (7) under the craft, and the moments of this wave to cause pitch and roll give the following forcing function vector:

$$\{F_w\} = \begin{Bmatrix} D_1 \\ D_2 \\ D_3 \\ D_4 \end{Bmatrix} \eta_o e^{i\omega_e t} \tag{10}$$

Assuming sinusoidal solutions of frequency ω_e of Eq. (1) with forcing functions Eq. (10) ratioed to wave amplitude Eq. (7) gives per unit wave amplitude

$$[-\omega_e{}^2[A] + i\omega_e[B] + [C]] \begin{Bmatrix} z/\eta_o \\ \theta/\eta_o \\ \varphi/\eta_o \\ m_{B/\eta_o} \end{Bmatrix} = \begin{Bmatrix} D_1 \\ D_2 \\ D_3 \\ D_4 \end{Bmatrix} \tag{11}$$

with

$$D_1 = K_{\theta D}/B + C_B A_B\ I_1 \tag{12}$$

$$D_2 = (K_{\theta D}/B)\ I_2 + C_B A_B (m - 0.5)L\ I_1 \tag{13}$$

$$D_3 = -(K_{\varphi D}/L)\ I_3 \tag{14}$$

$$D_4 = \rho_A (C_B R_1 + G/A_B) I_1 \tag{15}$$

Frequency Domain Solutions

Solutions of Eq. (11) as a function of encounter frequency ω_e give the transfer functions in heave z/η_o, pitch θ/η_o, roll φ/η_o, and cushion mass m_B/η_o. Auxiliary equation (5) may then be solved to give the cushion pressure perturbation transfer function P_B/η_o. The Response Amplitude Operators (RAO's) are the squares of the amplitudes of the abovementioned transfer functions. Acceleration RAO's are obtained by multiplying the heave, pitch, and roll RAO's by $\omega_e{}^4$. From an appropriate geometric matrix multiplication of the heave, pitch, and roll transfer functions, and squaring the result, gives the vertical motion (RAO's) at selected points on the craft. Multiplication of these RAO's by $\omega_e{}^4$ gives the vertical acceleration RAO's for the selected points.

Parameters Determined Experimentally

A basic assumption used in deriving the equations of motion is that cushion pitch and roll stiffness characteristics are distributed over the cushion in a manner analogous to that of a bedspring with a large number of identical coils. These characteristics are represented by the parameters $K_{\theta D}$ for pitch longitudinally distributed stiffness and $K_{\varphi D}$ for roll laterally distributed stiffness. This assumption allows the use of average cushion characteristics, but necessitates the utilization of empirical stiffness and damping information for the pitch and roll degrees-of-freedom.

Values of pitch and roll stiffness are established by determining the slope of a moment vs displacement plot derived analytically or from subscale model tests. The damping terms in pitch ζ_θ and ζ were determined by monitoring the decay in pitch and roll oscillatory response due to a step displacement perturbation applied to a subscale model. This assumes that pitch and roll response can be characterized by simple linear second-order systems.

Theoretical and Experimental Correlation

It was recognized during the development of the linearized seakeeping simulation that because an attempt was being made to linearize the characteristics of a fairly nonlinear system, a comparison between theoretically and experimentally derived craft motion was necessary before proceeding to a useful application of the analysis technique. Consequently, a fairly extensive model test program was conducted in which craft motions were accurately measured under controlled environmental conditions. These tests and the comparison of experimental and theoretical results are now discussed under the headings of "Time Domain Correlation" and "Frequency Domain Correlation," respectively.

Time Domain Correlation

Dynamic tests of a subscale model have been conducted at the Aerojet Sacramento Facility during which step functions in heave force, pitch moment, and roll moment were applied to a model (of 6 ft cushion length) while on-cushion at zero forward speed over a smooth and level hard surface. The resulting dynamic response in pitch, heave, and roll were recorded to provide the bases for the experimental evaluation of motion damping and damped natural frequency. Concurrently, a digital computer program was developed in which the linearized heave, pitch, roll, and cushion flow equations of the ACV digital seakeeping simulation were mechanized for solution in the time domain. The model and model test conditions were then simulated and the resulting time response was computed and compared with experimental results as shown in Fig. 2. As may be seen, the correlation between the assumed linear mathematical model and experiment was reasonably well established, with both frequency and damping sufficiently well simulated by a linear mathematical model. The heave transient was found to correlate least. The pitch was quite well represented by a linear second-order differential equation. The roll test data shows a departure from linearity near the end of the transient.

The major conclusion drawn from this comparison was that, utilizing experimental values of stiffness and damping, some modes of motion, i.e., pitch and, to some extent, roll, can be adequately represented by linear second-order differential equations.

Frequency Domain Correlation

The frequency domain simulation of air cushion vehicle dynamic behavior in a seaway is a powerful design and development tool. Because simulation results are based on statistical principles and mean response is predicted rather than lengthy time histories, the economical analysis of large number of operating conditions and configurations is possible. This feature is extremely important, since most air cushion vehicle operation occurs over terrain and in seas of random unevenness. Characterizing the dynamic response of a vehicle over such surfaces in the time domain would require a great deal of computational time for each condition in order to provide adequate statistical confidence in the results. Balanced against this advan-

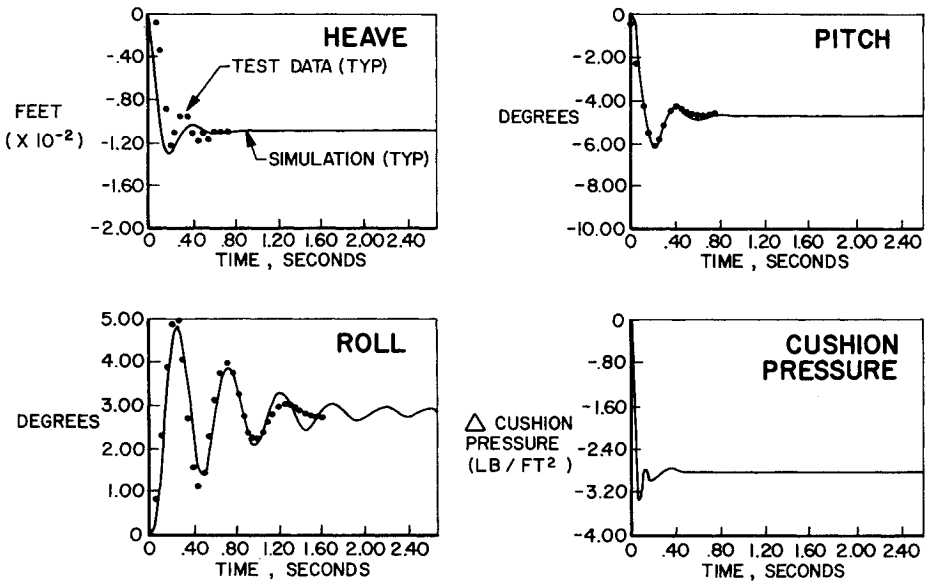

Fig. 2 Time domain correlations.

tage, however, is the fact that the form of simulation is limited to having linear mathematical relationships and that nonlinear characteristics occurring in large excursion motions, such as the closing off of skirt air gaps, cannot be properly taken into account. This is why verification of the analytical technique is sought through correlation with model tests.

Two bases for frequency domain correlation are used. The first is discussed in terms of the difference between experimental and theoretical response amplitude operators (RAO's), and the second in terms of a comparison of rms response. RAO's characterize craft behavior normalized to the excitation environment and are defined as the ratio of the square of the peak-to-peak response to the wave height squared, as a function of encounter frequency. They are determined experimentally by taking analog response data, digitizing it, and transforming it from the time domain to the frequency domain. The same process is followed with data for the seaway. The output squared is divided by the input to obtain RAO's. For a given set of operating conditions (e.g., airflow rate and model forward speed, etc.) the RAO's are ideally invariant with seaway spectra. This is illustrated in Fig. 3 which depicts the heave RAO's for several runs having the same significant wave height for a model ACV tested at a linear towing tank. Comparisons are made in model scale dimensions because the craft does not conform to Froude scaling laws.

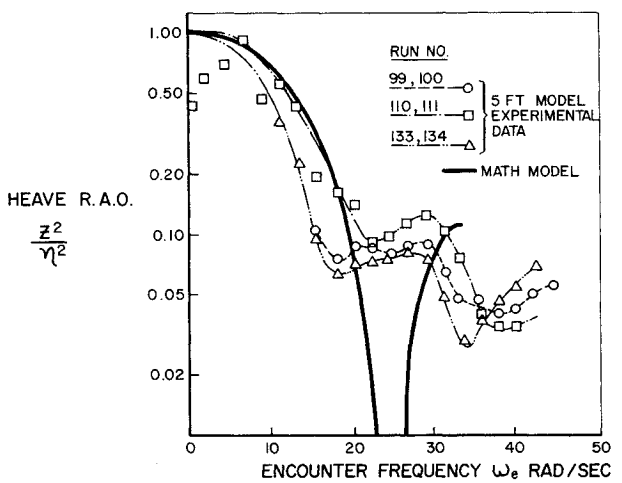

Fig. 3 Comparison of theoretical and experimental subscale model heave RAO in the encounter frequency domain. Model speed U_m, 15 fps, $H_{1/3}$ = 0.09 ft.

Scaling-up results could lead to misinterpretation of full-scale craft behavior as discussed later.

Two differences between the measured and predicted RAO's are common to all of the run conditions studied. One is that the predicted secondary peaks for the heave RAO's appear at slightly higher frequencies than those for the experimental RAO's. This is probably due to the choice of values used for the cushion dynamic parameters. The best available information was used in analyzing the lift system characteristics, and lift system parameters were not arbitrarily altered in order to fit the data.

The other major difference between measured and predicted RAO's is that the data does not indicate the sharp drop off in response at specific frequencies as are produced by the mathematical model. These decreases result because, theoretically, certain wavelengths produce no excitation force, and hence no response. The data does indicate local minima but the "valleys" are not as deep. This is to be expected since the experimental response output includes extraneous information ("noise") as well as the real response. Also, response from forces other than those produced by wave pumping and cushion air flow leakage variation (e.g., seal contact forces), will be present in the data output.

In general, the occasional large differences apparent at specific frequencies in these studies do not have a corresponding impact on over-all rms response, as will be shown below.

Results of a comparison of rms response vs craft speed for tests of a 6 ft model ACV at the Stevens Institute of Technology Laboratory are shown in Fig. 4. The crosses show the rms acceleration predicted by applying the measured tank wave spectrum (shown later in Fig. 7) to the simulation while the circles depict the corresponding accelerations determined by integrating acceleration measurements over the length of the run. Figure 4 is bow vertical acceleration for scaled Sea State 2 tests ($H_{1/3}$ = 0.16 ft).

Results show that the best over-all comparison is for run 102 where measured bow accelerations are nearly identical to the values predicted. It is interesting to note that for the higher speed cases there is more variation between measured results for runs of common conditions than between measured and predicted results. This is most apparent with the examination of rms bow acceleration response for runs 102 and 103. This is probably because the run length is insufficient to provide an adequate statistical sample.

Another significant trend is that of higher accelerations

at higher speeds. This results because accelerations tend to increase with the square of response frequency. Therefore, since wave encounter frequencies increase with increasing speed in head sea operation, accelerations are expected to increase also. This explanation is true so long as vehicle rigid body response frequencies are within the range of significant wave energy. If the speed becomes high enough, wave energy frequencies could be shifted above the region of receptiveness of the craft.

The trends indicated by measurements are followed quite well by the analysis. Where relatively large differences occur, they are at the higher speeds and indicate a tendency for over prediction on the part of the mathematical model.

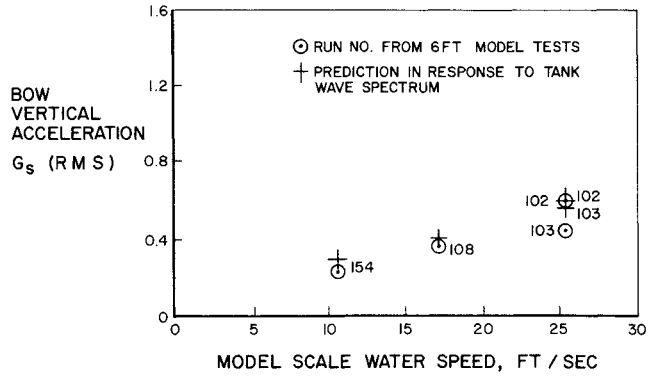

Fig. 4 Comparison of measured and predicted bow response of a 6 ft model ACV. Model heading into scaled Sea State 2.

Model Scale Effects

Laws of Dynamic Similarity

Often the most realistic and practical means of evaluating the performance of a dynamic system is by means of model testing where environmental conditions often can be easily controlled and model motion accurately measured. To gather by model experimentation an accurate representation of the dynamic behavior of a full-scale ACV in response to a seaway, however, normally requires a model and test facility which can duplicate geometrically and dynamically similar conditions as those existing at full scale. Much of the knowledge of ACV dynamic behavior has, in fact, been gained from such experimentation. If the model behavior under consideration justifiably can be assumed to be controlled primarily and dynamic similarity have been achieved the model test results can easily be converted to full scale merely by using the general laws of dynamic similitude. If the acceleration due to gravity is considered to be the same for the model and full-scale craft and if λ is the linear scale ratio (l_f/l_m), the scale factors for the model can be derived by taking mass M to vary as λ^3, length L as λ, and time T as $\lambda^{0.5}$. Thus, for example, response frequency which has dimensions of rad/sec will vary as $1/T$ or as $\lambda^{-0.5}$ and pitch damping which has units of LMT will vary as $(\lambda.\lambda^3.\lambda^{0.5})$ or $\lambda^{4.5}$.

Nevertheless, the model designer and test engineer are faced invariably with a difficult task even to approach correct dynamic similarity. Model characteristics which prove to be the most difficult to scale include the pressure and flow relationship of the air supply system, operating weight for low cushion pressure tests, and skirt material stiffness. Likewise, it is not easy to provide for a true representation of model test conditions. Seas, for example, cannot always be considered long crested and propagating in a direction parallel to the course of an ACV as is the normal case for a model responding to waves generated by a wave maker in a linear towing tank. Although there are many other model and test conditions which are difficult to represent, in general, they can be considered to be of second-order significance apart from one consideration, which will be discussed briefly.

Atmospheric Pressure Effects

Equation (1) described the dynamic equilibrium condition for heave, pitch, roll, and lift air mass flow. The linear stiffness matrix C of Eq. (1), given as Eq. (4) is shown to contain the cushion compressibility term C_B in every nonzero coefficient except that which governs roll, where $C_B = (\bar{p}_B + P_A)(\gamma/V_B)$, $\bar{p}_B$ = cushion pressure, P_A = atmospheric pressure, V_B = cushion volume, and γ = ratio of specific heats for air.

The significance of the contribution of this term is perhaps not fully recognized, however, until consideration is given to the requirement for obtaining true dynamic similarity during model testing. Since C_B is and $\bar{p}_B \ll P_A$, it is found that the cushion compressibility term C_B which scales as λ^{-2} can be considerably in error if atmospheric pressure is not also scaled for model test conditions.

The extent of possible distortions that may arise if atmospheric pressure were not scaled during model tests is explored in the Appendix. Here the linear characteristic equation of coupled heave and cushion airflow is developed in terms of the Laplace Transform Variable S [Eq. (A23)] for conditions in which heave motion is uncoupled from the pitch and roll. Solutions of this cubic polynominal [shown as Eq. (A23)] can then be obtained for model conditions in which atmospheric pressure is scaled and unscaled. The results, given in Fig. 5, show the variation in heave damping and damped natural frequency ascribed by the roots of Eq. (A23) solved for as a function of time average model lift airflow rate.

This figure readily shows that for unscaled atmospheric pressure the heave damping ratio (which is the cosine of the angle formed by the negative abscissa and a line intersecting the curve from the origin) decreases with increased airflow rate. However, if the atmospheric pressure is scaled down for model conditions, the damping ratio increases with increased lift airflow rate as shown by the broken curve of Fig. 5. Also, the level of damping for the model with unscaled atmospheric pressure is considerably higher than for the correctly scaled atmospheric pressure condition. It can be shown theoretically that for a full-scale craft, the damping increases with increased airflow rate. Thus, it is seen that if the atmospheric pressure were scaled from the full-scale craft just as for any other parameter, the model would then show the same trend (as far as airflow rate is concerned) as the full-scale craft.

This result is very important as far as ACV dynamic studies are concerned. The implication is that, tested with a full head of atmosphere, the fundamental cushion-coupled dynamic characteristics of a scale model are such that a considerably distorted picture of the heave damping expected in a full-scale craft is inherent in the model.

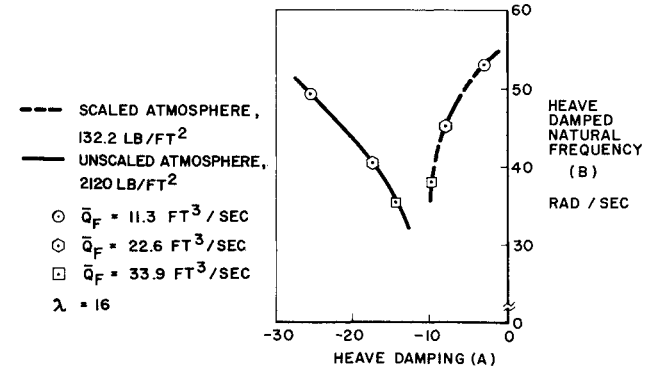

Fig. 5 Heave root migration. Heave damping ratio: $-\varphi_H = -A/(A^2 + B^2)^{1/2}$.

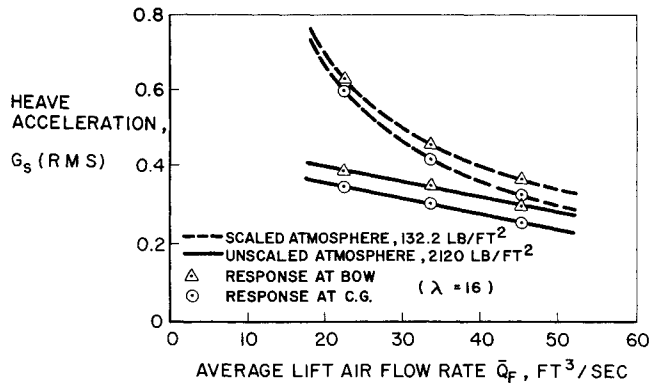

Fig. 6 Rms heave acceleration response of model ACV showing scale effects.

It will now be shown that as a result of nonscaling of atmospheric pressure, there is expected to be a significant distortion in the vertical acceleration response of a subscale model.

Figure 6 shows the predicted vertical acceleration response of a model at its bow and c.g. as a function of lift airflow rate for operation while heading into a scaled Sea State 2 described by a Pierson-Moskowitz Storm Spectrum. From Fig. 6 it is seen that by increasing lift airflow rate, the vertical acceleration response at the bow and c.g. decreases for both scaled and unscaled atmospheric pressure conditions, but the effect is much more pronounced for the scaled atmospheric condition. Also the acceleration response for the scaled atmospheric pressure condition is significantly higher at low airflow than that for the unscaled pressure condition.

The rapid decrease in acceleration response, with increase in airflow rate, for the scaled atmospheric pressure condition is primarily explained by the rapid increase in heave damping as shown in Fig. 5. However, although the heave damping is actually decreased with increased flow for the unscaled pressure condition, the acceleration response decreases. Acceleration response tends to vary in proportion to the square of the response frequency. Therefore, since the damped natural frequency is reduced with increasing flow rate for the unscaled atmospheric pressure condition, this effect offsets the reduction in damping and increased energy absorbed and results in a reduction in vertical acceleration response.

In summary, the distortion effects due to unscaled atmospheric pressure at subscale conditions is shown from mathematical simulation to produce the following major results and conclusions.

1) A subscale model can tend to produce heave accelerations which are less than those expected in a corresponding full-scale craft. Thus, full-scale predictions of heave dynamic response based on model tests must be carefully made while taking into account the expected distortion.

2) Parameters that significantly improve the dynamic behavior of a subscale model may not be as effective full scale. Likewise, methods of passive heave attenuation (such as increasing total lift air flow Q_F) that do not appear fruitful from model test results may prove more effective for a full-scale craft.

The aforementioned results suggest that ACV models, for true full-scale representation, should be tested under conditions where the effects of unscaled atmospheric pressure are compensated or eliminated.

Further specific experimental work along these lines is suggested as follows. 1) Conduct dynamic model tests in a wind tunnel where the atmospheric pressure and density can be controlled. 2) Test a simple piston-cylinder fixed area leakage representation of heave and cushion airflow dynamics and simulate variations in pressure and density.

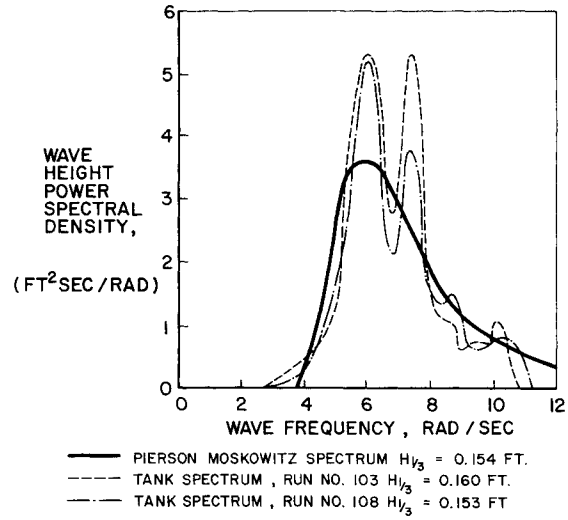

Fig. 7 Variance in model test wave spectra.

3) Run further tests in accordance with suggestion 2, when some controlled heave-dependent leakage flow is allowed. 4) Test two scale models having a relative scale ratio of at least 4, to provide experimental evidence of scaling distortion effects.

Simple analytic models of suggestions 2 and 3 are fairly easy to obtain. In fact for no heave dependent leakage ($a_o = 0$) and small d_z/M_c compared with $C_B R_1$, the characteristic polynominal from the Appendix, Eq. (23a), becomes

$$P(s) = S^2 - C_B R_1 S + C_B A_B{}^2/M_C$$

and

$$\omega_n = (C_B/M_C)^{1/2} A_B \qquad \zeta = -R_1 (C_B M_C)^{1/2}/2A_B \tag{16}$$

with

$$K_{\theta D} L << C_B A_B{}^2$$

Also, for the case where the adiabatic stiffness $C_B A_B{}^2$ is large compared to the mass of the model, the cubic term in $P(s)$ may be neglected and, in fact, the natural frequency or damping no longer depends on C_B. For this case, the heave dependent leakage is retained, and the characteristic polynominal is

$$P(s) = S^2 - (A_B{}^2 - d_z R_1/M_c R_1)\, S - A_B G/M_c R_1$$

and

$$\omega_n = (-A_B G/M_c R_1)^{1/2} \tag{17}$$

$$\zeta = [A_B{}^2 - d_z R_1]/[2(-A_B G M_c R_1)^{1/2}]$$

Equations (16) and (17) supply some physical significance to the parameters that affect craft dynamics for some special cases that could be experimentally investigated by the models of suggestions 2 and 3.

Prediction of Full-Scale Acceleration Response

Comparison of Simulated and Experimentally Determined Full-Scale Response

The problem associated with model scale effects discussed previously are apparent when comparisons are made between measured subscale model response and that predicted for a corresponding full-scale craft. Ideally, the acceleration response measured on a dynamically similar model should be used as a direct measure of the response of the full-scale craft. Unfortunately, perfect representation of an idealized seaway condition in the model basin is difficult even without the inherent problem of achieving true model similitude. For example, a plot of a

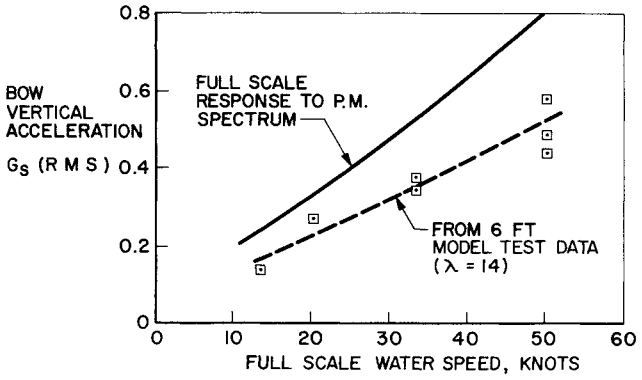

Fig. 8 Comparison of model bow response to that predicted at full scale for operation into Sea State 2.

scaled-down Pierson-Moskowitz seaway is compared in Fig. 7 with the measured seaway spectra actually achieved in the towing tank. This figure shows a significant discrepancy between actual and ideal spectra.§ For these reasons, therefore, model test seaway spectra were used basically to verify the mathematical simulation at model scale, as previously described.

Figure 8 presents a comparison between predicted full scale vertical accelerations in response to a Pierson-Moskowitz (PM) spectrum and the vertical acceleration of a 6 ft model in response to an actual towing tank spectrum having approximately the same scaled significant height.

These figures are presented in order to emphasize the fact that scaling model test data directly to full scale can lead to erroneous predictions of full-scale craft dynamic response. The major causes of error include: 1) nonscaling of atmospheric pressure as discussed previously, 2) differences in spectral content of towing tank and full-scale design spectrum, 3) difficulties in obtaining true models of a) the air supply system, b) all inertia properties in the same model, and of c) miscellaneous geometrical and physical constraints imposed by model testing.

Figure 8 applies to a particular ACV for which scaling model test data to full scale predicts acceleration response significantly lower than mathematical model predictions of full-scale craft response. This would generally be the case insofar as the result is related to nonscaling atmospheric pressure. The second and third causes of error listed may have the effect of either increasing or decreasing acceleration response, depending on the actual specific conditions. The implication is that care must be exercised to simulate carefully the design wave spectra, if model test data is to be scaled up for design uses. Also, care and perhaps considerable expense must be involved to overcome some of the physical difficulties associated with obtaining true scaled experimental models and operating conditions of ACV's.

Design Tradeoff Considerations

It is during the preliminary phases of an ACV design that the analytic techniques described in this paper can be used to the greatest advantage. If proper consideration is given to craft dynamic behavior early enough, then even if compromises are made, they are made with the full knowledge of the consequences which will arise with regard to ride quality and structural seakeeping loads.

There are not many gross design variables of an ACV which do not have a bearing upon craft dynamic behavior. As a result, it is practical to discuss here just a few of the most significant. One of the most influential tradeoff considerations and one which is often used to help identify lift power and lift system air supply characteristics is that which involves the conflicting requirements for static and dynamic stability.

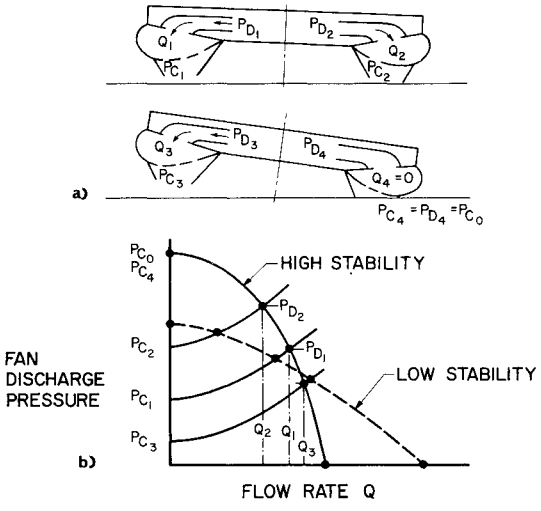

Fig. 9 Static stability dependence upon lift system characteristics.

In general, it is found that when static heave, pitch, and roll stability is increased with the objective of increasing craft speed tolerance to c.g. shift, to increase a crafts' resistance to plow-in and overturn, or to reduce the probability of hard structure impact in a seaway, a corresponding degradation in ride quality and an increase in the level of seakeeping loads will occur. Static stability is measured in terms of the resistance offered by the cushion system to static changes in heave, pitch, and roll displacement. For pitch and roll this is most effectively gained in the skirt noncontact regime by compartmentation of the skirt system (see Fig. 9a) and in the positive skirt contact regime by providing for a favorable geometric shift in the center of cushion area as a function of angular displacement. With careful skirt design, extremely high orders of static stability are possible but not without an air supply system having a delivery pressure sensitive to changes in airflow rate (see Fig. 9b). It is this relationship between static stability and the air supply characteristic which is one of the considerations in the selection of type and design of air moving device, whether it be an axial flow, mixed flow, or radial flow impeller system.

To proceed with an explanation of the design tradeoff in question, it is convenient to reduce the problem to an evaluation of the relationship between three basic design variables.

1) The design lift airflow rate which, for a craft of given weight, air distribution system, and air moving device will completely dictate lift power requirements.

2) Lift system maximum static pressure rise (occurring at close to zero flow) which, in conjunction with the design lift airflow rate, will tend to control the characteristic (pressure) head-flow relationship of the supply system and the sensitivity of discharge pressure with respect to changes in air flow rate.

3) Bow and c.g. vertical acceleration in response to a prescribed sea state which may be considered to strongly influence ride quality and structural loading.

Figure 10 presents the results of a typical parametric study. Here the vertical acceleration response for a craft of given weight and geometry in terms of g's is shown as a function of delivered airflow rate, cutoff pressure ratio,¶

§It has come to the author's attention that the indicated discrepancy may have been caused by improper spectral analysis of the actual model data, rather than by the achievement of a true experimental PM seaway.

¶The ratio of zero flow pressure to normal design static delivery pressure as depicted in Fig. 9b.

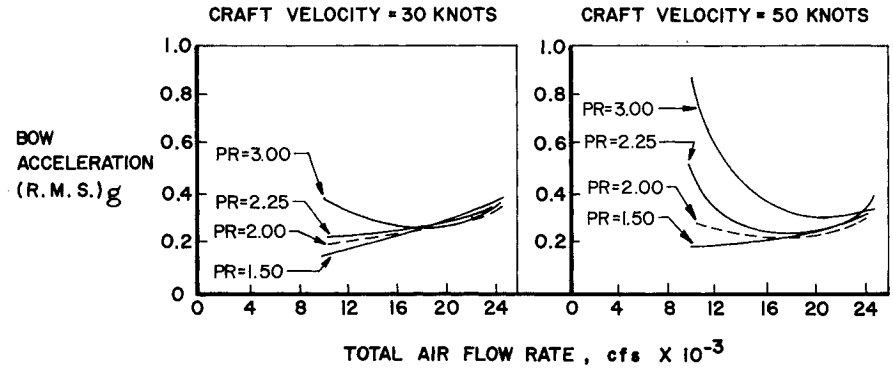

Fig. 10 Lift system parameter variation effect upon bow acceleration response; *PR* = cutoff pressure ratio.

and forward speed while heading into a particular sea state. The irregularity of the curves indicate the complex interaction between the pitch and heave components of total response as the pitch and heave natural frequencies shift toward and away from resonance. For the particular example considered, it is seen that high lift system cutoff pressure (i.e., high static stability) leads to high levels of acceleration response, particularly at low levels of airflow rate.

Increasing lift airflow rate in most cases eventually leads to an optimum flow rate giving minimum response for a particular cutoff pressure. The procedure is therefore to: 1) identify a cutoff pressure ratio to give satisfactory static stability based upon criteria developed to assess craft's resistance to overturn or drag sensitivity to c.g. shift; and 2) identify a design speed and, for a given sea state, select a flow rate to give minimum response. The results then provide the means to identify lift power requirements and lift system head flow characteristics. The tradeoff between static stability and dynamic response cannot be fully exercised, however, until a criterion is obtained which governs acceptable levels of acceleration.

Structural Loads

Seakeeping loads

Internal stress loads for the purpose of structural design are usually computed in the form of longitudinal and transverse distributions of shear force and bending moment, and corresponding distributions of torsional moment. For Eq. (18), the mass of the craft is considered to be distributed uniformly plus concentrated weights at discrete intervals. Another restricting assumption is that the mass of the craft is symmetric with respect to the transverse centerline. (These conditions are closely true in practical designs.) The longitudinal distributed forces in the linearized system are of the form

$$I_{TOT} = m_c(\ddot{z} - \xi\ddot{\theta}) + \sum_{j=1}^{i} (W_j/g)\, I(x_j)(\ddot{z} - x_j\ddot{\theta}) + (d_z/L)\,(\dot{z} - \xi\dot{\theta}) + K_{\theta D}(z - \xi\theta) + (A_B)/L)P_B$$

$$f(\xi) = -(K_{\theta D}/B)\, 2\eta_o/k_y \sin(k_y B/2)\, e^{-i(k_x \xi - \omega_e t)} \qquad (18)$$

$$I(x_j) = \begin{cases} 1, & x = x_j \\ 0, & x \neq x_j \end{cases} \qquad x_j \leq x_i$$

where W_j is the longitudinal discrete weight at longitudinal station and m_c, the uniform mass per unit length of craft.

The applied force per unit length is the second relation of Eq. (18) and is denoted by $f(\xi)$ with the first relation of Eq. (18) being the dynamic reaction denoted by I_{TOT}. Thus, the distributed loading ratioed to the input wave amplitude η_0 is

$$p(\xi)/\eta_o = f(\xi)/\eta_o - I_{TOT}/\eta_o \qquad (19)$$

The distributed longitudinal shear is given by

$$\frac{V_x}{\eta_o} = \int_{-\ell_s}^{x} \frac{p(\xi)}{\eta_o}\, d\xi \qquad (20)$$

The distributed longitudinal bending moment is given by

$$\frac{M_B(x)}{\eta_o} = \int_{-\ell_s}^{x} \frac{V(\xi)}{\eta_o}\, d\xi \qquad (21)$$

The transverse distributed forces per unit beam of the craft are

$$J_{TOT} = \frac{m_c L}{B}(\ddot{z} + \eta\ddot{\varphi}) - \frac{m_c}{B} L^2(m - 0.5)\,\ddot{\theta} + \sum_{s=1}^{r} \frac{W_s}{g} I(y_s)(\ddot{z} + y_s\ddot{\varphi}) - \ddot{\theta} \sum_{s=1}^{r}\sum_{j=1}^{n} \frac{W_{sj}}{g}\, x_j I(y_s) + \frac{d_z}{B}(\dot{z} + \eta\dot{\varphi}) - \frac{d_z L}{B}(m - 0.5)\,\dot{\theta} + \frac{K_{\varphi D}}{B}(z + \eta\varphi) - \frac{K_{\theta D}}{B} L^2(m - 0.5)\theta + \frac{A_B}{B} P_B$$

$$f(\eta) = -\frac{K_{\varphi D}}{L}\frac{\eta_o}{k_x}(\psi - i\,\phi)e^{-i(k_y \eta - \omega_e t)} \qquad (22)$$

$$I(y_s) = \begin{cases} 1, & y = y_s \\ 0, & y \neq y_s \end{cases} \qquad y_r \geq y_s$$

where W_s is the transverse discrete weights at transverse station y_s and m_c, the uniform mass per unit length of craft.

Analogous to Eq. (19), the transverse load distribution is

$$p(\eta)/\eta_o = f(\eta)/\eta_o - J_{TOT}/\eta_o \qquad (23)$$

with distributed transverse shear given by

$$\frac{V(y)}{\eta_o} = \int_{-B/2}^{y} p(\eta)/\eta_o\, d\eta \qquad (24)$$

and distributed transverse bending moment

$$\frac{M_B(y)}{\eta_o} = \int_{-B/2}^{y} V(\eta)/\eta_o\, d\eta \qquad (25)$$

The longitudinal distributed torsional moment is given by

$$K_{TOT} = \left[\frac{m_c B^2}{12} + \sum_{s=1}^{m} \frac{W_{sj}}{g} y_{sj}^2 I(x_j)\right]\ddot{\varphi} + \frac{d_\varphi}{L}\dot{\varphi} + \frac{K_{\varphi D}}{L}\frac{B^3}{12}\varphi \qquad (26a)$$

$$n(\xi) = -\frac{K_{\varphi D}}{L}\frac{\eta_o}{k_y} i B\left(\cos\frac{k_y B}{2} - \frac{2}{k_y B}\sin\frac{k_y B}{2}\right)e^{-i(k_\xi \xi - \omega_e t)} \qquad (26b)$$

where

$$W_j = \sum_{s=1}^{m} W_{sj}$$

W_j is the transverse summing of discrete weight at longitudinal station x_j, and W_{sj} is the transverse station(s) of weight at longitudinal station x_j

Denoting Eq. (26b) by $n(\xi)/\eta_0$ per unit wave amplitude η_0 and the dynamic reaction [Eq. (26a)] by K_{TOT}/η_0, the distributed torsional moment is given by

$$T(\xi)/\eta_o = n(\xi)/\eta_o - K_{TOT}/\eta_o \tag{27}$$

The torsional moment as a function of longitudinal coordinate (x) is given by

$$\frac{T(x)}{\eta_o} = \int_{-\ell_s}^{x} \frac{T(\xi)}{\eta_o}\, d\xi \tag{28}$$

The boundary conditions for all internal loads are stated for longitudinal distributions as:

$$V(-\ell_s)/\eta_o = M_B(-\ell_s)/\eta_o = T(-\ell_s)/\eta_o = 0 \tag{29}$$

and

$$V(\ell_b)/\eta_o = M_B(\ell_b)/\eta_o = T(\ell_b)/\eta_o = 0 \tag{30}$$

and for lateral distributions as:

$$\frac{V(-B/2)}{\eta_o} = \frac{M_B(-B/2)}{\eta_o} = 0 \tag{31}$$

and

$$\frac{V(B/2)}{\eta_o} = \frac{M_B(B/2)}{\eta_o} = 0 \tag{32}$$

Boundary conditions (29) and (31) are automatically satisfied in the various load equations derived from Eqs. (20, 21, 24, 25, and 28). The longitudinal shear boundary condition $V(l_b)/\eta_0 = 0$ is satisfied inherently by the first of Eqs. (1) with wave forcing functions Eq. (10) constituting the right-hand side of Eq. (1). This is the heave force balance equation. The torsional moment boundary equation $T(l_b)/\eta_0 = 0$ is satisfied inherently by the third of Eqs. (1) with wave forcing functions Eq. (10) constituting the right-hand side of Eq. (1). This is the roll moment balance equation. The transverse shear boundary condition $V(B/2)\eta_0 = 0$ is satisfied only for the restricted case $K_{\varphi D}/L = K_{\theta D}/B$. The longitudinal bending moment boundary condition $M(l_b)/\eta_0 = 0$ is satisfied because the summation of moments about any point of a system in dynamic equilibrium is zero. The same is true of the transverse bending moment for the restricted case mentioned in connection with the transverse shear.

Additional relationships needed to insure compatibility between the loads equations and the equations of dynamic equilibrium are

$$\left.\begin{aligned} M_c &= m_c L + \sum_{j=1}^{n} \frac{W_j}{g} = m_c L + \sum_{s=1}^{m} \frac{W_s}{g} \\ I_\theta &= \frac{m_c L^3}{3}(1 - 3m + 3m^2) + \sum_{j=1}^{n} \frac{W_j}{g} x_j^2 \\ I_\varphi &= \frac{m_c L B^2}{12} + \sum_{j=1}^{n}\sum_{s=1}^{m} \frac{W_{sj}}{g} y_s^2 \end{aligned}\right\} \tag{33}$$

where n is the total number of discrete weights in longitudinal distribution and m, the total number of discrete weights in transverse distribution.

The loads equations are transformed to the encounter frequency domain, and loads transfer functions are determined in terms of heave, pitch, roll, cushion mass, and cushion pressure transfer functions. Loads (RAO's) are then determined from the square of the amplitudes of the loads transfer functions. For a given wave spectrum, sea state (in terms of significant wave heights $H_{1/3}$), and craft forward velocity, the mean square internal load distributions are then calculated utilizing a computer program. Static internal loads are also calculated and the absolute value of static load and a factor times the rms dynamic load can be summed. Examples of longitudinal bending moment for a typical craft are shown in Fig. 11. The factor K_σ used for these distributions was 3. This was considered the limit load condition for design purposes. Slamming load distributions, which now will be discussed, and also other load conditions are shown for comparison purposes in Fig. 11.

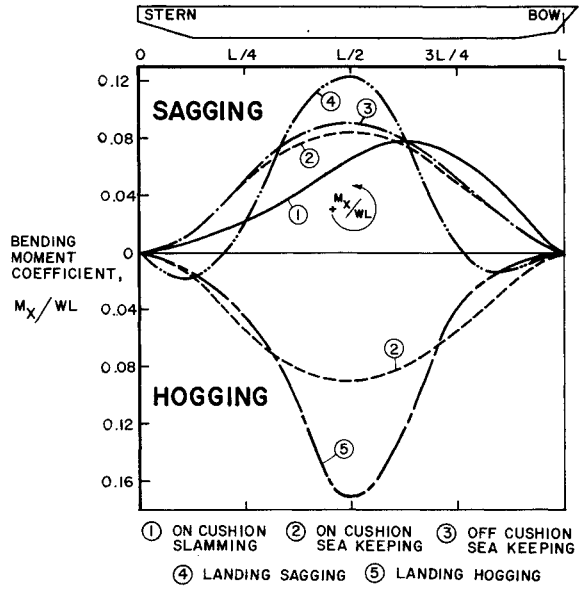

Fig. 11 Longitudinal structural load distributions.

Slamming loads

As an air cushion vehicle proceeds in the on-cushion mode in a seaway, the hard structure which forms the bow is normally well clear of the water. However, because of the irregular surface of the sea and the pitch, heave, roll motions of the craft, it is inevitable that the bow will occasionally come into contact with the water. The loads and their probability of occurrence generated by these events are a critical factor in the structural design of the craft. The linear seakeeping model provides basic and necessary information in the consideration of slamming effects of calculating the frequency of occurrence of water contact at or above a critical relative velocity, as well as average relative motion (to the water surface) at hard structure points of interest.

The joint probability P_{SJO} that hard structure point i will be immersed below the normal water surface h_{ci} and have a downward relative slam velocity of v_{si} is

$$P_{SJO} = 1/4\ [\text{erfc}\ h_{ci}/(2)^{1/2}\sigma_i][\ \text{erfc}\ v_{si}/(2^\sigma)_i^{1/2}] \tag{34}$$

Equation (34) is based on the analysis of the probabilistic characteristics of slamming as described in Ref. 1.

The frequency of occurrence of slams on a given bow location h_{ci} at or above a given threshold relative slamming velocity v_{si} was given in Refs. 2 and 3, as

$$FSB_i = \omega_i/2_\pi \exp -1/2\ \{1/\sigma i^2[h_{ci}^2 + (v_{si}/\omega_i)^2]\} \tag{35}$$

A general procedure can be adopted to calculate a bow impact load acting on a craft assuming that the motion of the craft, prior to the bow impacting on the wave surface, is defined by the craft dynamic response simulation, and to superimpose on this motion, the motion which is due to the load on the bow. This assumption infers that the contact of the bow with the water surface is a relatively rare event, compared with the effective frequency of relative motion.

The reaction of a craft to a bow impact load can be assumed to be totally that due to inertia, since no significant damping forces are expected to develop during the relatively short time interval of an impact. A step-by-step method of calculation can then be used in which the geometry and relative position of the craft to the wave is calculated at small time intervals and the accelerations and velocities integrated to give the velocities and displacements, respectively, for all six rigid body motion degrees of freedom.

The details of slamming loads analysis techniques are beyond the scope of this paper but the resulting long-term probability of bending moment due to slamming for a typical ACV is included as an example in Fig. 11. For a detailed discussion of the computational procedure and theory for calculating slamming forces and their induced shear force and bending moment.[4-6]

VII. Conclusions

The significant conclusions that can be made regarding the use of mathematical and subscale experimental models for predicting the dynamic behavior of full-scale ACV's are as follows.

1) Design of full-scale craft can usually employ both subscale experimental models and linearized mathematical models jointly in the representation of vertical plane dynamics.

2) Reliance on scaled-up model test data (obtained under normal atmospheric pressure conditions) alone can lead to erroneous conclusions regarding ride comfort, dynamic response, and loads of full-scale craft primarily because of the usual nonscalability of atmospheric pressure.

3) The analysis technique presented shows an acceptable correlation with actual model dynamic behavior to insure its usefulness as a design tool.

4) The early utilization of this dynamic analysis technique allows important ACV design parameters to be evaluated in terms of effects on stability, structural design, and ride comfort.

Recommended further experimental and analytical studies are as follows.

1) Conduct dynamic model tests in a wind tunnel where the atmospheric pressure can be controlled. Response to periodic or random surfaces could possibly be mechanized by means of a traveling belt.

2) Experimentally investigate simple piston-cylinder-fixed area leakage and subsequent controlled heave-dependent leakage models at normal atmospheric pressure and compare them with simplified analytical models.

3) Test two scale models having a relative scale ratio of at least 4 to provide experimental evidence of the scaling distortion effects.

4) Study, analytically, the effect of differences between long-crested and short-crested seas.

Appendix

Nonlinear Heave, Pitch, Roll, and Cushion Equations of Motion

Consider the ACV shown schematically in Fig. 1. The balance of heave forces and moment on the craft assume a rectangular cushion area of length L and beam B giving area $A_B = BL$. The following equations for sinusoidal wave excitation are then derived from Newton's laws:

Heave

$$M_c\ddot{Z} - M_c g + p_B A_B + d_z\dot{Z} + K_{\theta D}L[Z - (m - 0.5)L\Theta] = - (K_{\theta D}/B)\eta_o I_1, e^{i\omega_e t} \quad \text{(A1)}$$

where

$$\ell_b = mL, \quad \ell_s = (1 - m)L$$

Pitch

$$I_\theta\ddot{\Theta} - A_B L(m - 0.5)p_B + d_\theta\Theta + K_\theta\Theta = (K_{\theta D}/B)\,\eta_o I_2 e^{i\omega_e t} \quad \text{(A2)}$$

Roll

$$I_\varphi\ddot{\phi} + d_\varphi\dot{\phi} + K_\varphi\phi = - (K_{\varphi D}/L)\,\eta_o I_3 e^{i\omega_e t} \quad \text{(A3)}$$

Evaluating the preceding integrals gives

$$I_1 = \int_{-\ell_s}^{\ell_b}\int_{-\frac{B}{2}}^{\frac{B}{2}} e^{-i(k_x x + k_y y)}dy\,dx = \begin{cases} \dfrac{2}{k_x k_y}\sin\dfrac{k_y B}{2}\,(\Psi - i\Phi), & k_x, k_y \neq 0 \\ \dfrac{2L}{k_y}\sin\dfrac{k_y B}{2}, & k_x = 0,\ k_y \neq 0 \\ \dfrac{B}{k_x}(\Psi - i\Phi), & k_x \neq 0,\ k_y = 0 \\ BL = A_B, & k_x = k_y = 0 \end{cases} \quad \text{(A4)}$$

where

$$\Phi = 2\sin(k_y L/2)\sin k_x(\ell_b - \ell_s)/2$$

$$\Psi = 2\sin(k_x L/2)\cos k_x(\ell_b - \ell_s)/2$$

$$I_2 = \int_{-\ell_s}^{\ell_b}\int_{-\frac{B}{2}}^{\frac{B}{2}} x e^{-i(k_x x + k_y y)}dy\,dx = \begin{cases} (2/k_x k_y)\sin(k_y B/2)\,[\ell_b \sin k_x\ell_b - \ell_s \sin k_x\ell_s + i(\ell_b \cos k_x\ell_b + \ell_s \cos k_x\ell_s) - (1/k_x)(\Phi + i\Psi)]; & k_x,\ k_y \neq 0 \\ (B/k_x)[\ell_b \sin k_x\ell_b - \ell_s \sin k_x\ell_s + i(\ell_b \cos k_x\ell_b + \ell_s \cos k_x\ell_s) - (1/k_x)(\Phi + i\Psi)]; & k_x \neq 0,\ k_y = 0 \\ (1/k_y)\sin(k_y B/2)\,(\ell_b^2 - \ell_s^2); & k_x = 0,\ k_y \neq 0 \\ B(m - 0.5)L^2; & k_x = k_y = 0 \end{cases} \quad \text{(A5)}$$

$$I_3 = \int_{-\ell_s}^{\ell_b}\int_{-\frac{B}{2}}^{\frac{B}{2}} y e^{-i(k_x x + k_y y)}dy\,dx = \begin{cases} (\Psi - i\Phi)\dfrac{i}{k_x}\left(\dfrac{B}{k_y}\cos\dfrac{k_y B}{2} - \dfrac{2}{k_y^2}\sin\dfrac{k_y B}{2}\right); & k_x,\ k_y \neq 0 \\ Li\left(\dfrac{B}{k_y}\cos\dfrac{k_y B}{2} - \dfrac{2}{k_y^2}\sin\dfrac{k_y B}{2}\right); & k_x = 0,\ k_y \neq 0 \\ 0 & ;\ k_x \neq 0,\ k_y = 0 \\ 0 & ;\ k_x = k_y = 0 \end{cases} \quad \text{(A6)}$$

And cushion equations:

Mass of Air in Cushion

$$\dot{M}_B = \rho_B(Q_F - Q_{LS} - Q_{LO}) \quad \text{(A7)}$$

Air Density

$$\rho_B = M_B/V_B \quad \text{(A8)}$$

Cushion Volume

$$V_B = V_O - A_B Z + (m - 0.5)A_B L\Theta - \eta_o I_1 e^{i\omega_e t} \quad \text{(A9)}$$

Fan Flow Rate

$$Q_F = F_1 + F_2 p_B + F_3 p_B^2 \quad \text{(A10)}$$

Fixed Area Leakage

$$Q_{LO} = C_{DO}A_{LO}(2|\bar{p}_B|/\rho_B)^{1/2}\,\mathrm{sgn}\,\bar{p}_B \quad \text{(A11)}$$

where sgn $\bar{p}_B$ is the sign of cushion nominal gage pressure $\bar{p}_B$ plus if greater than atmospheric, minus if less than atmospheric.

Heave Dependent Leakage

$$Q_{LS} = \{C_{DS}C[-Z + (m-0.5)L\Theta] - (C_{DS}C/A_B)\eta_o I_1 e^{i\omega_e t} \times (2|\bar{p}_B|/\rho_B)^{1/2} \operatorname{sgn}\bar{p}_B\} \quad \text{(A12)}$$

In the dynamic dependent leakage equation (A12) the inherent assumption is that the craft tends to follow the wave contour to the extent that the net hover gap is always greater than zero. This is, of course, a very limiting assumption, since in practical situations the leakage gap is intermittently closed off (at least partially) as waves pass under the craft. Experience with models has shown that the dynamic dependent leakage area is not simply described in terms of the changes in hover gap, but upon the complex relative deformations of the individual cells allowing air to escape between them. The problem of accurately simulating, mathematically, the complex dynamic dependent leakage mechanism is currently being addressed by the authors.

Adiabatic Cushion Compression

$$(\bar{p}_B + P_A) = \text{const}\ \rho_B{}^{\gamma} \quad \text{(A13)}$$

The quantities $K_{\theta D}/B$ and $K_{\varphi D}/L$ are distributed effective air cushion stabilizing springs associated with a peripheral cell skirt design. $K_{\theta D}$ is the longitudinally distributed spring for pitch stabilization and $K_{\varphi D}$ is the transversely distributed spring for roll stabilization. These parameters were determined from model test data. The damping coefficient d_θ was also determined from test data, and represented as a longitudinally distributed damper.

Because of the distributed damper analogy, it is necessary to consider this damper to be effective in heave and roll as well as the measured value in pitch in order that the forces and moments due to the distributed damper be compatible in the heave, pitch, and roll equations. This is of fundamental importance in considering external load distributions for the purpose of generating internal (shear and bending moment) loads.

The compatible values of distributed heave damping d_z and transversely distributed roll damping d_φ were obtained from d_θ as

$$\left.\begin{aligned} d_z &= (3d_\theta/L^2)\ 1/1 - 3m + 3m^2 \\ d_\varphi &= d_z B^2/12 \end{aligned}\right\} \quad \text{(A14)}$$

In order to insure loads compatibility between longitudinal and transverse distributions for the distributed spring forces it was necessary to insure that

$$K_{\theta D}/B = K_{\varphi D}/L \quad \text{(A15)}$$

Actual model tests have indicated that (A15) is approximately true.

Linearized and Reduced Equations of Motion

Equations (A1–A13) were linearized by a linear perturbation technique, where the perturbation variables were expressed as

$$\left.\begin{aligned} Z &= \bar{Z} + z \\ \Theta &= \bar{\Theta} + \theta \\ \phi &= \bar{\phi} + \varphi \\ M_B &= \bar{M}_B + m_B \\ p_B &= \bar{p}_B + P_B \end{aligned}\right\} \quad \text{(A16)}$$

where z, θ, φ, m_B and P_B are linear perturbations about the nominal values $\bar{Z}$, $\bar{\Theta}$, $\bar{\Phi}$, $\bar{M}_B$, and $\bar{p}_B$ of heave, pitch, roll cushion air mass, and cushion pressure, respectively.

Employing Eq. (A16) in Eqs. (A1–A13), and making use of the integrals (A14–A16), we obtain the reduced linearized equations

$$[A]\begin{Bmatrix}\ddot{z}\\ \ddot{\theta}\\ \ddot{\varphi}\\ \ddot{m}_B\end{Bmatrix} + [B]\begin{Bmatrix}\dot{z}\\ \dot{\theta}\\ \dot{\varphi}\\ \dot{m}_B\end{Bmatrix} + [C]\begin{Bmatrix}z\\ \theta\\ \varphi\\ m_B\end{Bmatrix} = \eta_o e^{i\omega_e t}\begin{Bmatrix}D_1\\ D_2\\ D_3\\ D_4\end{Bmatrix} \quad \text{(A17)}$$

The matrices $[A]$, $[B]$, and $[C]$ and the forcing function vector

$$\begin{Bmatrix}D_1\\ D_2\\ D_3\\ D_4\end{Bmatrix}$$

are given in the main body of this paper as relations (2–4, 10). In addition we obtain the pressure perturbation equation in terms of the other variables as

$$P_B = (C_B/\rho_A)m_B + C_B A_B z - C_B A_B(m-0.5)L\theta + C_B\eta_o I_1 e^{i\omega_e t} \quad \text{(A18)}$$

The following important constants appearing in Eq. (A17) are defined as follows:

Adiabatic Stiffness

$$C_B = (\bar{p}_B + P_A)\gamma/V_B$$

(P_A = atmospheric pressure)

Fan Conductance

$$\left.\begin{aligned} R_1 &= F_2 + 2F_3\bar{p}_B - \bar{Q}_F/2\bar{p}_B \\ &= F_c - \bar{Q}_F/2\bar{p}_B \end{aligned}\right\} \quad \text{(A19)}$$

Fan $(\partial QF/\partial p_B)$ Characteristic Slope

$$F_c = F_2 + 2F_3\bar{p}_B$$

Heave Dependent Leakage Parameter

$$G = C_{DS}C(2\bar{p}_B/\rho_A)^{1/2}$$

Assumptions made in linearization are

$$\bar{p}_B \ll P_A \quad \text{(A20)}$$

which implies $\bar{\rho}_B \approx \rho_A$. Hence

$$\frac{P_B}{\bar{p}_B} - \frac{\Delta\rho_B}{\rho_A} = \frac{P_A\gamma}{\bar{p}_B\rho_A}\left[1 - \frac{\bar{p}_B}{\rho_A\gamma}\right]\Delta\rho_B$$

where $\rho_B = \bar{\rho}_B + \Delta\rho_B$. Now $\bar{p}_B/p_A\gamma \ll 1$ so that

$$\frac{P_B}{\bar{p}_B} - \frac{\Delta\rho_B}{\rho_A} \approx \frac{P_A\gamma}{\bar{p}_B\rho_A}\Delta\rho_B = \frac{P_B}{\bar{p}_B}$$

and $\Delta\rho_B/\rho_A \approx 0$.

Characteristic Equation of Uncoupled Linear Heave-Cushion Flow System in Laplace Transform Variable(s)

For the condition $m = 0.5$, which implies that the c.g. of the craft is longitudinally at the center of the cushion, the linear equations in heave and pitch become uncoupled, so that we may consider only the simultaneous solution of the heave and cushion flow equation.

$$\begin{bmatrix}M_c & 0\\ 0 & 0\end{bmatrix}\begin{Bmatrix}\ddot{z}\\ \ddot{m}_B\end{Bmatrix} + \begin{bmatrix}d_z & 0\\ 0 & 1\end{bmatrix}\begin{Bmatrix}\dot{z}\\ \dot{m}_B\end{Bmatrix} + \begin{bmatrix}K_{\theta D}L + C_B A_B{}^2 C_B A_B/\rho_A\\ -\rho_A(C_B A_B R_1 + G) - C_B R_1\end{bmatrix}\begin{Bmatrix}z\\ m_B\end{Bmatrix} = \eta_o e^{i\omega_e t}\begin{bmatrix}D_1\\ D_4\end{bmatrix} \quad \text{(A21)}$$

Letting $\eta(t) = \eta_0 e^{i\omega e^t}$ and obtaining the Laplace transform of Eq. (A21) with zero initial conditions, we obtain the heave transfer function

$$z(s)/\eta = (b_1 s + b_0)/a_3 s^3 + a_2 s^2 + a_1 s + a_0) \quad \text{(A22)}$$

where

$$a_3 = 1 \qquad b_1 = -\frac{1}{M_c}\left(\frac{K_{\theta D}}{B} + C_B A_B\right) I_1$$

$$a_2 = d_3/M_c - C_B R_1 \qquad b_0 = \frac{C_B I_1}{M_C}\left(R_1 \frac{K_{\theta D}}{B} - G\right)$$

$$a_1 = \frac{K_{\theta D} L + C_B (A_B{}^2 - d_z R_1)}{M_c}$$

$$a_0 = \frac{C_B (A_B G - K_{\theta D} L R_1)}{M_c}$$

The cubic polynominal equation

$$P(s) = a_3 s^3 + a_2 s^2 + a_1 s + a_0 = 0 \quad \text{(A23)}$$

is the characteristic equation of the system and Eq. (A22) is the heave transfer function $z(s)/\eta$.

References

[1]Vassilopoulos, L., "The Analytical Prediction of Ship Performance in Random Seas Including a New Correlation of Theoretical and Experimental Model Motions in Regular Waves," Ph.D. thesis, Feb. 1964, Dept. of Naval Architecture and Marine Engineering, MIT, Cambridge, Mass.

[2]Ochi, M. K., "Prediction of Occurrence and Severity of Ship Slamming at Sea," Fifth Symposium on Normal Hydrodynamics, Office of Naval Research, USA, and Ships Model Tank, Norway, Bergen, Norway, 1964.

[3]Tick, L. J., "Certain Probabilities Associated with Bow Submergence and Ship Slamming in Irregular Seas," *Journal of Ship Research*, June 1958, pp. 30-36.

[4]Band, E. G. U., "Water Loads on the C-150-50 Landing Craft," Working Paper 18011-3, Sept. 1970, Payne Div., Wyle Labs., Rockville, Md.

[5]Band, E. G. U., "Calculation of Cushion-Borne Impact Loads on the JEFF(A) Landing Craft," Rept. E1303, Aug. 1971, Aerojet-General Corp., Tacoma, Wash.

[6]Chuang, S. L., "Impact Pressure Distribution on Wedge-Shaped Hull Bottoms of High-Speed Craft," Rept. 2953, Aug. 1969, Naval Ship Research and Development Center, Washington, D.C.

JULY 1974 J. HYDRONAUTICS VOL. 8, NO. 3

Systems Identification: Application to Underwater Vehicle Dynamics

B. E. Sandman* and J. G. Kelly†

Naval Underwater Systems Center, Newport, R.I.

A deterministic method of systems identification is presented in a generalized form applicable to numerous lumped-parameter mathematical models. The minimization of a measured error between experimental and calculated time records results in the optimum or best-fit model parameters and constitutes the basic identification process. The iterative search method suggested for optimization does not necessitate a good initial parameter estimate. The procedure is exemplified by an application to the governing equations of motion for an underwater vehicle. The hydrodynamic coefficients form the set of parameters for optimization. Coefficient retrieval using a theoretically generated record and the prediction of coefficient values from experimental records is investigated. The problem of numerical sensitivity is sighted. Although coefficients are determined for excellent agreement in the trajectories, a refined approach is suggested to reduce the number of parameters and improve the efficiency of search.

Nomenclature

x, y, z	=	body axes of vehicle
x_g, z_g	=	distances from CB to CG
$\delta_e(t)$	=	elevator input
U	=	magnitude of translational velocity
α	=	angle of attack
w	=	transverse component of velocity
θ	=	angle of pitch
m, W	=	mass and weight of vehicle, respectively
l	=	length of vehicle
B	=	buoyant force
ρ	=	mass density of fluid medium
I_y	=	moment of inertia about y-axis
Z', M'	=	hydrodynamic coefficients with respect to forces and moments
Z_o	=	depth of vehicle at CB
$\bar{x}$	=	state vector
$\bar{x}_c$	=	computed solution to motion equations
$\bar{x}_e$	=	experimental record of state
$\bar{x}_o$	=	initial-value vector
t	=	independent time variable
$\bar{\eta}$	=	(10×1) vector of hydrodynamic coefficients
ϵ	=	objective error function
$\{\ \}$	=	denotes a column vector
$[\ ]$	=	denotes a row vector
$\bar{\eta}^0$	=	vector of initial estimates
$\bar{\eta}^*$	=	denotes the value of $\bar{\eta}$ for a minimal ϵ
ϕ	=	(4×10) null matrix

Received August 3, 1973; revision received February 28, 1974.

Index categories: Marine Vessel Systems, Submerged; Marine Vessel Trajectories, Stability and Control

†Systems Analysis Staff.

*Systems Analysis Staff. Associate Member AIAA.

Introduction

THE analytical prediction of the dynamic response of an underwater vehicle is a function of a set of parameters commonly referred to as hydrodynamic coefficients. For a given body configuration, reasonable numerical estimation of these parameters is required for any accurate simulation of vehicle performance. Water tunnel tests, theoretical predictions, and trial-and-error adjustments of the coefficients of motion to obtain an observed numerical simulation of experimental records constitute the existing